A Numerical Simulation Study of SiGe/Si-Heterostructured PMOS and Bipolar Devices

J. B. Kuo, B. Y. Chen, H. P. Chen, T. C. Lu, and J. H. Sim
Rm. 526, Microelectronics Lab. Dept. of Electrical Eng.
National Taiwan University
Roosevelt Rd. Sec. 4 #1, Taipei, Taiwan 106-17
Fax:886-2-363-8247, Telephone:886-2-363-5251 x285
Email:jbkuo@cc.ee.ntu.edu.tw

Abstract

This paper reports a numerical simulation study of SiGe/Si heterostructured PMOS and bipolar devices using a modified 2D device simulation program. As confirmed by published data, the numerical simulation provides a good prediction on the IV characteristics for the SiGe-channel PMOS device and the f_T for the SiGe-based bipolar device.

Summary

SiGe/Si heterostructures have been applied to conventional PMOS and bipolar devices to enhance their speed performance [1]-[5]. How to optimize the SiGe/Si heterostructures is very important in designing advanced VLSI PMOS and bipolar devices. For PMOS devices, SiGe/Si heterostructure has been used to produce a quantum well such that transconductance can be improved [1]-[3]. For bipolar devices, SiGe/Si heterostructure has been used in the base region to enhance current gain and unity gain frequency [4][5]. For advanced SiGe/Si-heterostructured PMOS and bipolar devices, doping and germanium profiles in the active region may be complicated. Designing SiGe/Si-heterostructured PMOS and bipolar devices using device numerical simulation can be helpful. Recently, analysis of a SiGe-based bipolar device using device simulators has been reported [6][7]. In this paper, using a 2D device simulator, a numerical simulation study of SiGe/Si heterostructured PMOS and bipolar devices is described.

In order to conduct numerical analysis of the SiGe/Si heterostructured PMOS and bipolar devices, the PISCES program [8] has been modified to include the germanium-induced bandgap narrowing phenomenon. In the modified PISCES program, in addition to the heavy doping induced bandgap narrowing, the SiGe induced bandgap narrowing has been included. shows the cross section of the SiGe-channel PMOS device [2][3] under study. An $N+$ polysilicon gate with an oxide thickness of $120\mathring{A}$ is used. Below the gate oxide, a silicon cap of $50\mathring{A}$ is placed atop the undoped SiGe-channel of $200\mathring{A}$. Below the SiGe-channel, the substrate doping density is $1 \times 10^{16} cm^{-3}$. The S/D junction depth is $0.1\mu m$. In order to simplify the analysis, no interface charges are assumed.

Fig. 2 shows the I_D vs. V_{GS} characteristics of the SiGe-channel PMOS device with a germanium concentration of $0.15, 0.2, 0.25$. The drain-to-source voltage is $V_{DS} = -0.1V$. For a large germanium concentration, the threshold voltage shifts toward the positive direction as a result of an increase in the effective intrinsic carrier concentration. In addition, in the subthreshold region, all three cases show a similar n ($n = 1.214$), the normalized inverse subthreshold slope, which is defined as S ($S = 2.3 \cdot n \cdot \frac{kT}{q}$) of gate bias swing required to change to the subthreshold current by a factor of 10. At $V_{GS} = -0.8V$, for a germanium content changing from 0.15 to 0.2 and from 0.2 to 0.25, the drain current increases more than 5 times. For a more negative V_{GS}, the difference in the drain current among three cases gets smaller. Fig. 3 shows the internal hole density distributions in the substrate direction in the center of the SiGe-channel PMOS device with a germanium concentration of $0.15, 0.2, 0.25$ at $V_{GS} = -1V, -2V, -3V$ and $V_{DS} = -0.1V$. As shown in Fig. 3, at $V_{GS} = -1V$, the buried SiGe-channel dominates in all three cases. An increase in the germanium content leads to a large increase in hole density. Specifically, at $V_{GS} = -1V$ as shown in dotted lines, for a germanium content of 0.15, 0.2, and 0.25, the peak hole density in the SiGe buried channel is $9.48 \times 10^{15} cm^{-3}$, $3.07 \times 10^{16} cm^{-3}$, and $7.19 \times 10^{16} cm^{-3}$, respectively. At $V_{GS} = -2V$, as indicated in dashed lines in Fig. 3, although the buried SiGe-channel still dominates, the hole density in the silicon surface is not negligible. At $V_{GS} = -3V$, as shown in solid lines, the hole density at surface exceeds that in the buried SiGe-channel— the surface channel is the dominant conduction channel. In addition, the peak hole density in the buried channel is already saturated— A further decrease in V_{GS} does not provide an increase in hole density in the buried SiGe-channel [2]. Furthermore, the difference in the hole density profile among three cases is small. As a result, the drain current at a more negative V_{GS} looks similar among three cases.

Fig. 4 shows the doping and germanium profiles in the intrinsic region of the SiGe-based bipolar device [9]. The heterojunction bipolar device has a base width of $600\mathring{A}$, a peak base doping density of $2.5 \times 10^{18} cm^{-3}$, an emitter depth of $0.12\mu m$, a peak emitter doping density of $1 \times 10^{20} cm^{-3}$, and a $1.5 \times 10^{17} cm^{-3}$ epi-collector region of $0.7\mu m$. The germanium profile has a peak concentration of 8% as shown in Fig. 4. In order to simplify the analysis, poly-emitter structure is not included in the current device structure.

Fig. 5 shows the f_T vs. I_C curves for the SiGe-based bipolar device with and without germanium using the PISCES results and experimental data [9]. As shown in solid line, the PISCES simulation results indicate a good match with the experimental results. With germanium, the bipolar device shows a 2x advantage in peak f_T. Fig. 6 shows the f_T vs. germanium concentration of the SiGe-based bipolar device with a linearly-graded germanium profile based on the PISCES simulation and Kroemer's model results [10]. The SiGe-based bipolar device under study has identical characteristics as the one shown in Fig. 4 except the germanium profile — a linearly graded profile instead of a trapezoidal shape as shown in Fig. 4 has been used. In addition, the peak germanium location is at the base-collector junction, where the base transit time is the shortest [10]. As shown in Fig. 7, for a peak germanium concentration from 0 to 0.2, a close match between the PISCES simulation results and the Kroemer's analytical model results can be observed.

References

[1] D.Nayak et.al, *IEEE Symp on VLSI Tech*, Japan, 5/91
[2] P.Garone et.al, *IEEE EDL* 5/91
[3] P.Garone et.al, *IEDM* 12/90
[4] A.Pruijmboom et.al., *IEEE EDL* 7/91
[5] M. Ugajin,et.al, *IEEE BCTM*,92
[6] B. Pejcinovic, et.al, *IEEE TED* 9/92
[7] J.Chen et.al, *Sol St Elect*, 8/92
[8] J.Kuo et.al, *IEEE TED*, 2/92
[9] R.People, *Phys Rev.* 85
[10] H. Kroemer, *Sol St Elect*, 85

VIII. Figure Captions

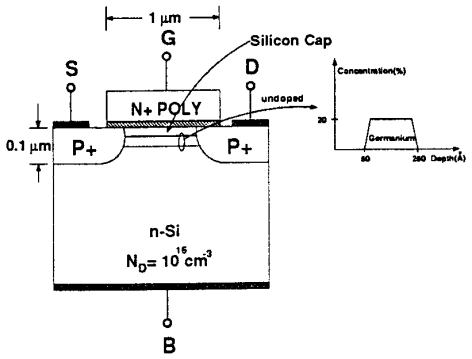

Fig. 1. Cross section of the SiGe-channel PMOS device under study.

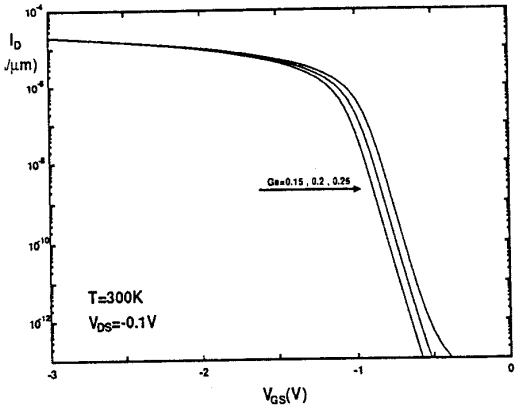

Fig. 2. The I_D vs. V_{GS} characteristics of the SiGe-channel PMOS device

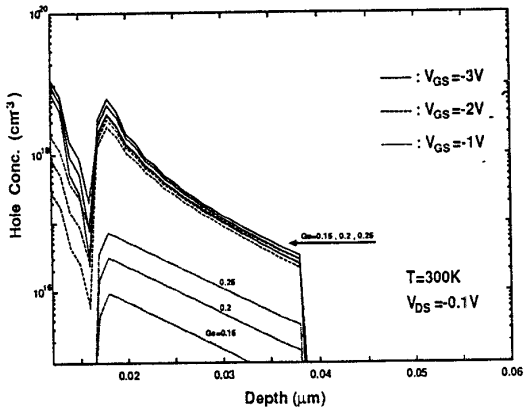

Fig. 3. The internal hole density distributions in the in the substrate direction in the center of the SiGe-channel PMOS

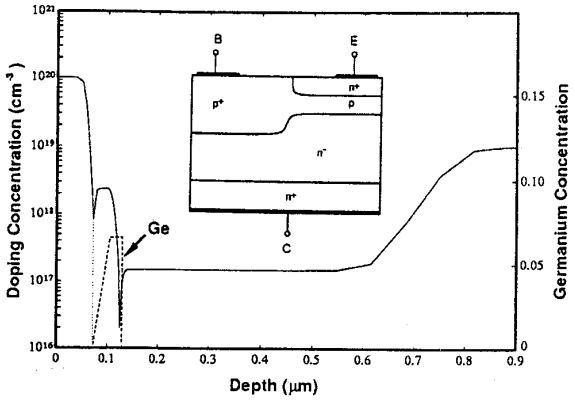

Fig. 4. Doping and germanium concentration profiles in the intrinsic region in the SiGe-based bipolar device.

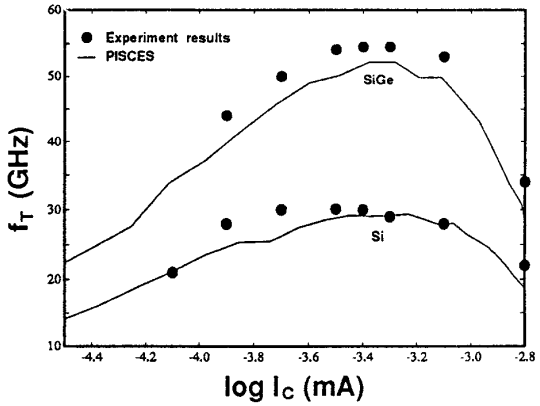

Fig. 5. The f_T vs. I_C curves of the BJT device with and without germanium

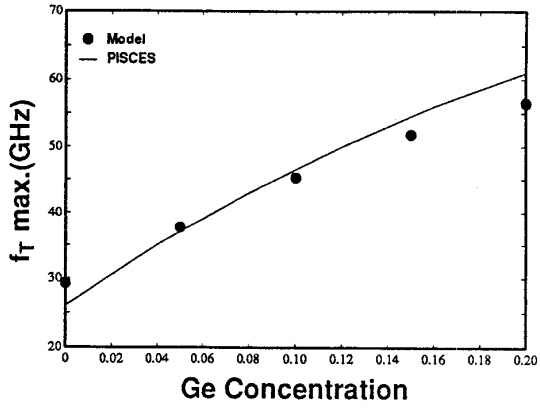

Fig. 6. f_T vs. germanium concentration of the SiGe-based bipolar device with a linearly-graded germanium profile based on the PISCES simulation and Kroemer's model results [10].